

Materials and processing aspects of CoCrTa/Cr longitudinal recording media. I. Processing and magnetic properties

Y. Shen^{a),b)} D. E. Laughlin,^{a)} and D. N. Lambeth^{c)}

Carnegie Mellon University, Pittsburgh, Pennsylvania 15213 Road, Fremont, California 94539

(Received 12 March 1993; accepted for publication 16 August 1994)

In this study, we correlate various processing conditions with the magnetic properties of CoCrTa/Cr films by varying the substrate preheating, the substrate bias, and the composition of the magnetic target. High H_c CoCrTa/Cr films with thin Cr underlayers were produced by either preheating the substrate or by rf bias sputtering. We found that the sputtering temperature of the magnetic layer plays a far more important role in reducing intergranular exchange coupling and increasing H_c than does the CoCrTa/Cr crystallographic texture. The optimum condition for preparing high H_c films depends on the magnetic target composition. Even though the crystallographic texture does not control H_c , it does have an effect on the ΔM curve which is related to the noise properties of CoCrTa/Cr media. ΔM measurements indicate that $\{1\bar{1}01\}_{\text{Co}}/\{110\}_{\text{Cr}}$ textured films may have slightly better noise properties than the films with $\{1120\}_{\text{Co}}/\{200\}_{\text{Cr}}$ texture with similar H_c . © 1994 American Institute of Physics.

I. INTRODUCTION

Sputtered CoCrTa/Cr films have recently been developed as one of the major commercial high performance longitudinal recording media for high density magnetic recording. It has been reported recently that thin Cr underlayers have a smoother surface, and consequently lead to a better recording performance.¹ With thin Cr underlayers (~ 500 Å), high H_c CoCrTa films have been fabricated by either substrate heating or bias-sputtering.^{1,2} The understanding of the H_c enhancement through substrate heating or bias-sputtering, however, is not complete. In the recording media industry, a number of processing conditions are often varied simultaneously during optimization. Consequently, many microstructural and materials features, such as crystallographic texture, grain size, segregation, and stress state change simultaneously and therefore their effects cannot be related directly to the magnetic properties. It is therefore important to design experiments to separate these effects and determine their individual roles in controlling the magnetic properties of thin film media.

In this study, we have correlated various processing conditions, in particular substrate preheating, substrate bias, and the target composition, with the resulting microstructure and magnetic properties of the CoCrTa/Cr films. In this article, we limit our discussion to the processing and magnetic properties of the CoCrTa/Cr media. In a latter paper,³ the microstructural aspects of the CoCrTa/Cr films will be presented so that a more comprehensive picture of the interrelationship among processing-microstructure-magnetic properties can be obtained.

II. EXPERIMENTAL PROCEDURES

The films in our study were rf sputtered onto 7059 Corning glass as well as onto circumferentially textured NiP/Al substrates in a LH Z-400 sputtering system. Two magnetic targets, namely, $\text{Co}_{82.8}\text{Cr}_{14.6}\text{Ta}_{2.6}$ and $\text{Co}_{86}\text{Cr}_{12}\text{Ta}_2$ were chosen in order to illustrate the composition effect on the magnetic properties. The base pressure of the sputtering chamber was 7×10^{-7} Torr. We fixed the Ar pressure at 10 mTorr during sputtering with a forward power density of 2.5 W/cm². At these conditions, the deposition rates of Cr and CoCrTa were 10 and 14 nm per minute, respectively.

Hysteresis loops were obtained in a vibrating sample magnetometer (VSM) with saturation fields of 10 kOe. ΔM measurements were also conducted to examine the magnetic intergranular interactions in these films. Such measurements have been shown to be related directly to the signal to noise properties in magnetic recording media.^{4,5} The maximum field used to obtain the ΔM curves is $2.5H_c$ of the films. The film stress was obtained by using a technique developed by Glang *et al.*⁶ After magnetic characterization, these films were examined by x-ray diffraction (Rigaku, $\text{Cu } K\alpha$) to obtain structural information.

III. RESULTS AND DISCUSSION

A. Effect of Cr underlayer thickness

Figure 1 shows a plot of H_c vs Cr underlayer thickness (t_{Cr}) for the low Co concentration target ($\text{Co}_{82.8}\text{Cr}_{14.6}\text{Ta}_{2.6}$) when neither substrate heating nor biasing was employed. The thickness of 400 Å for the magnetic layer was chosen for this composition because a sufficient signal for recording tests can be produced ($M_s t \approx 2.0$ memu/cm²). Consistent with earlier results,⁷ the H_c increases with the Cr underlayer thickness. However, the highest H_c obtained is less than

^{a)}Department of and Materials Science and Engineering.

^{b)}Read-Rite Corporation 44100 Osgood Rd., Fremont, CA 94539.

^{c)}Department of Electrical and Computer Engineering.

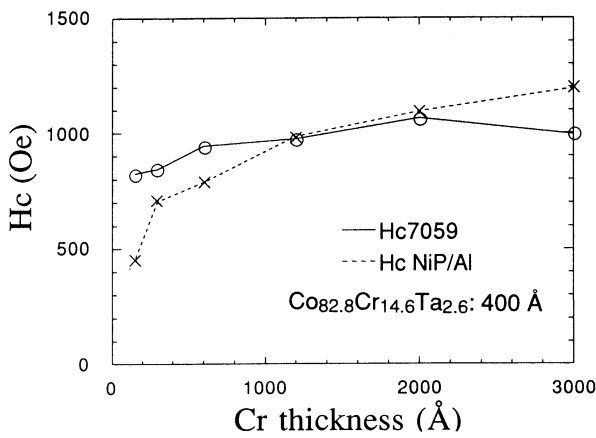


FIG. 1. The dependence of H_c of $\text{Co}_{82.8}\text{Cr}_{14.6}\text{Ta}_{2.6}(400 \text{ \AA})/\text{Cr}$ films on Cr thickness (t_{Cr}) without substrate heating or biasing.

1200 Oe. In order to obtain higher H_c CoCrTa/Cr films, either substrate preheating or rf bias sputtering is required.

B. The effect of substrate preheating

The dependence of H_c and crystallographic texture of CoCrTa/Cr films on T_{sub} has been reported for the cases where both the Co and Cr layers are deposited at the same T_{sub} .^{8,9} As T_{sub} increases, the crystallographic texture of the bilayer films changes from the $\{1101\}_{\text{Co}}/\{110\}_{\text{Cr}}$ to the $\{1120\}_{\text{Co}}/\{200\}_{\text{Cr}}$. Thus, the increase in H_c with T_{sub} could be caused by either the change in the crystallographic texture of the CoCrTa film or by other microstructural changes such as grain size, defect structure, and/or increased segregation of nonmagnetic constituents. It is therefore impossible to determine which controls H_c more, the crystallographic texture or one of the other T_{sub} induced effects.

In order to separate the effects of crystallographic texture from those of elevated T_{sub} , we have fabricated films as shown schematically in Fig. 2. We first deposited the Cr underlayer at 260 °C thereby obtaining the $\{200\}$ texture. The Cr film was then cooled to room temperature and the CoCrTa film was deposited on the $\{200\}$ Cr after a soft bias etch was performed. This enables us to obtain a CoCrTa film with the $\{1120\}$ texture deposited at room temperature (sample B).

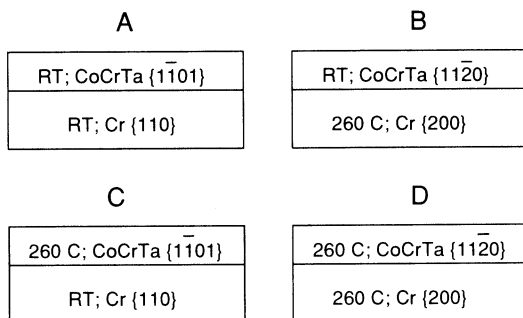


FIG. 2. A schematic of four $\text{Co}_{82.8}\text{Cr}_{14.6}\text{Ta}_{2.6}(400 \text{ \AA})/\text{Cr}$ samples designed to separate the crystallographic texture from other temperature induced effect on the magnetic properties of CoCrTa/Cr films.

Conversely, we also obtained the $\{1101\}$ textured CoCrTa film (sample C) at elevated T_{sub} by first depositing the Cr underlayer at room temperature and then heating the substrate to 260 °C before the CoCrTa film was deposited [Fig. 2(c)]. When both layers were deposited at room temperature or 260 °C, we designate the films as samples A and D, respectively. By comparing samples C with D and A with B one can determine the effect of crystallographic texture on the magnetic properties of the films. Similarly, by comparing specimens B with D and A with C the effect of T_{sub} on the magnetic properties of the films can be deduced.

Table I lists the crystallographic texture, sputtering temperature of the magnetic layer, and magnetic properties of these four films made from the low Co concentration target ($\text{Co}_{82.8}\text{Cr}_{14.6}\text{Ta}_{2.6}$). It is evident that H_c was much higher for both Cr textures when a CoCrTa layer was deposited at elevated temperature. On the other hand, for the same magnetic layer temperature, the improvement in H_c due to crystallographic texture change is less than 15%, with the $\{1120\}_{\text{Co}}/\{200\}_{\text{Cr}}$ textured films having a higher H_c than the $\{1101\}_{\text{Co}}/\{110\}_{\text{Cr}}$ textured films. This combination of samples shows that the enhancement of H_c in the CoCrTa/Cr films is mainly due to the elevated T_{sub} . Either of the textures is acceptable.

Even though H_c of the CoCrTa/Cr films appears to be almost independent of the Cr underlayer texture, the texture does affect S^* and thus may affect the noise properties. In order to examine this, ΔM curves were measured to assess the magnetic intergranular interaction in these films. It is commonly believed that a positive ΔM corresponds to intergranular exchange coupling. Minimum intergranular coupling is generally desired for low noise media.^{4,5} Figure 3 shows the ΔM curves for each of the films. There appears to be a strong intergranular exchange interaction in the CoCrTa films deposited at room temperature [Fig. 3(a)]. As the sputtering temperature of the magnetic layer was raised to 260 °C, the exchange interaction was markedly reduced [Fig. 3(b)]. For the films with the same sputtering temperature of the magnetic layer, our experimental results showed that the $\{1101\}_{\text{Co}}/\{110\}_{\text{Cr}}$ films have a lower ΔM than the $\{1120\}_{\text{Co}}/\{200\}_{\text{Cr}}$ films at both room temperature and 260 °C. This suggests that the $\{1101\}_{\text{Co}}/\{110\}_{\text{Cr}}$ texture would be preferred for better signal/noise media.

Recently, Tsai *et al.*¹⁰ reported that $\{1120\}_{\text{Co}}/\{200\}_{\text{Cr}}$ textured films had better recording characteristics. In their study, both the crystallographic texture and the sputtering temperature of the magnetic layer were varied simultaneously corresponding to our samples A and D. Thus, their results are consistent with ours up to that point. Our contribution is to have shown that the crystallographic texture effect on magnetic properties was overwhelmed by the sputtering temperature induced effect. Thus, we have demonstrated that it is important to have the same sputter temperature of the magnetic layers in order to assess the effect of crystallographic texture on H_c and on recording characteristics.

Lu *et al.* also attempted¹¹ to distinguish effects of crystallographic texture and substrate temperature on magnetic properties. Unfortunately, it was very difficult to obtain complete crystallographic texture information due to interference

TABLE I. T_{sub} , crystallographic texture and magnetic properties of four samples prepared according to the scheme shown in Fig. 2.

Sample A					
400 Å (Co,RT)/600(Cr,RT)					
Substrate	H_c	S	S^*	C_{texture}	C_{Otexture}
Glass	945	0.86	0.86	110	$\bar{1}\bar{1}01$
NiP/Al	788	0.83	0.91	110	$\bar{1}\bar{1}01$
Sample B					
400 Å (Co,RT)/300(Cr,RT)300(Cr,260 C)					
Glass	1005	0.85	0.91	200	$1\bar{1}\bar{2}0$
NiP/Al	796	0.85	0.94	200	$1\bar{1}\bar{2}0$
Sample C					
400 Å (Co,260 C)/600(Cr,RT)					
Glass	1452	0.72	0.74	110	$\bar{1}\bar{1}01$
NiP/Al	1662	0.90	0.74	110	$\bar{1}\bar{1}01$
Sample D					
400 Å (Co,260 C)/600(Cr,260 C)					
Glass	1532	0.78	0.83	200	$1\bar{1}\bar{2}0$
NiP/Al	1752	0.92	0.88	200	$1\bar{1}\bar{2}0$

of Al x-ray diffraction peaks arising from the Al/NiP disk substrates. No evidence of the full epitaxial growth of the magnetic layer was presented in their paper, as no soft-etching on the underlayer was performed when the underlayer and magnetic layer were deposited at different temperatures.

B. Role of the Cr underlayer in forming CoCrTa crystallographic texture

The importance of obtaining appropriate crystallographic texture in the magnetic layer is associated with the magnetocrystalline anisotropy. By introducing a Cr underlayer, a favorable crystallographic texture is developed in Co based recording media, in which the easy magnetic c axis lies in or nearly in the film plane. Three orientational relationships have been observed in Co/Cr bilayer films,^{9,12} namely,

$$\text{Pitsch-Schrader: } \{1\bar{1}\bar{2}0\}_{\text{Co}}/\{200\}_{\text{Cr}}, [0002]_{\text{Co}}/[1\bar{1}\bar{1}]_{\text{Cr}};$$

$$\text{Potter: } \{1\bar{1}01\}_{\text{Co}}/\{110\}_{\text{Cr}}, [1\bar{2}10]_{\text{Co}}/[1\bar{1}\bar{1}]_{\text{Cr}};$$

$$\text{Burgers: } \{1\bar{1}\bar{2}0\}_{\text{Co}}/\{111\}_{\text{Cr}}, [0002]_{\text{Co}}/[10\bar{1}]_{\text{Cr}}.$$

The origin of such orientation relationships is the reduction of the excess surface energy through optimum atomic matching of the Co and Cr structure across the interface. Clean Cr surfaces are necessary for the Co films to grow epitaxially. Consequently, the key to growing certain textured Co films at different sputtering temperatures is to obtain the corresponding Cr underlayer texture and to maintain a clean Cr surface.

Our L.H. Z-400 sputtering system employed a resistive heater. Heating the substrate from room temperature to 260 °C took approximately 45 min, while cooling from 260 °C to room temperature occurred overnight in vacuum. To ensure a clean Cr surface after 45 min heating, we applied a low power etching prior to depositing the Co layer. Figure 4 shows the H_c dependence on the etching power for sample C on the NiP/Al substrate. When the etching power exceeded 0.3 W/cm² for a fixed etching time (2 min), H_c reached a

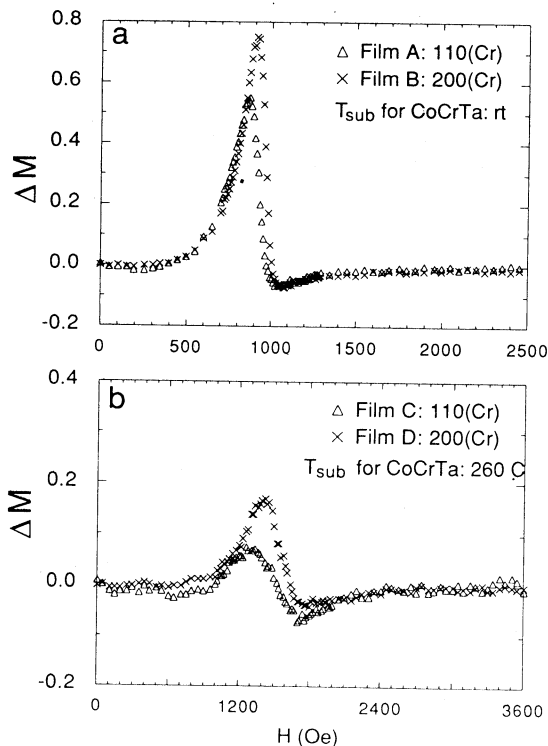


FIG. 3. ΔM curves for CoCrTa/Cr films on glass substrate.

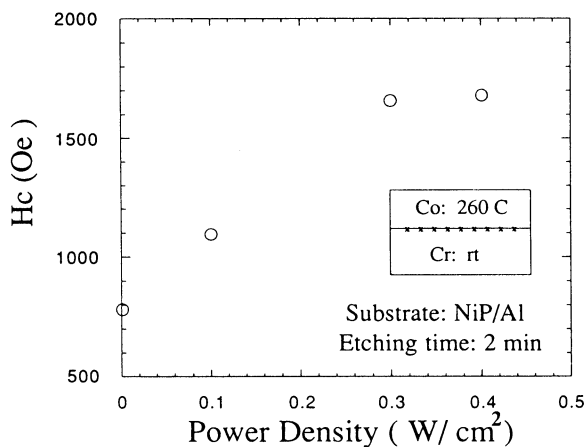


FIG. 4. H_c dependence of CoCrTa(400 Å, 260 °C)/Cr(600 Å, room temperature) on the etching power applied to Cr before the deposition of the CoCrTa.

plateau. A clean Cr surface was presumably obtained after this etching, demonstrating the importance of a clean Cr surface in order to achieve optimum H_c .

In the absence of etching between deposition of the layers, a {0002} crystallographic texture developed in the CoCrTa layer, as displayed in Fig. 5(b), in the 400 Å (Co,RT)/600 Å (Cr,260 °C) film. Since cooling took considerably longer time than heating, a larger sputter etching power was essential to clean the Cr surface in order to ensure the development of the {11 $\bar{2}$ 0} crystallographic texture. See Fig. 5(a). To avoid the heating effect induced by sputter etching, a split Cr underlayer of sample B was made with the first 300 Å Cr underlayer deposited at the elevated temperature and the remainder at room temperature. In this case, no etching was required between deposition of the Cr layers to obtain {11 $\bar{2}$ 0} textured CoCrTa film sputtered at room temperature [Fig. 5(c)].

C. Bias-sputtering of the Cr layer only and the substrate effect

Figure 6(a) displays a plot of H_c of CoCrTa/Cr films deposited on glass substrates versus rf bias voltage. The rf bias sputtering was employed only during the deposition of the Cr layer. There is a similarity in the H_c dependence between the CoCrTa films deposited by bias sputtering on the Cr underlayer and by preheating the substrate [Fig. 6(b)]. In the LH Z-400 sputtering system, both the glass and NiP/Al were placed on a stainless steel base plate. For this configuration, we found, however, that the enhancement in H_c due to bias sputtering of the Cr layer on NiP/Al was much smaller than the enhancement of H_c when sputtered onto the Corning glass. See Table II.

During bias sputtering of the Cr underlayer, the constant Ar ion bombardment on the substrate caused the substrate to heat. In addition, a longer sputtering time was required to compensate for the decrease in sputtering rate for a fixed sputtering power since a constant Cr thickness was desired. This further enhanced the substrate heating due to the bias. Like the Corning glass, NiP also has an amorphous structure

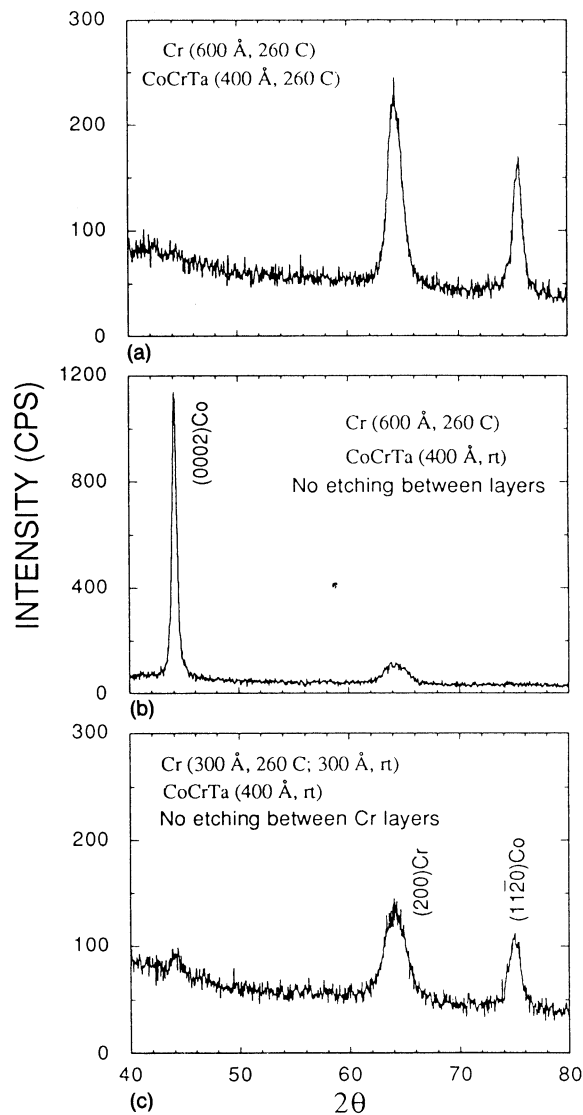


FIG. 5. X-ray spectra of films prepared as follows: (a) CoCrTa(400 Å, 260 °C)/Cr(600 Å, 260 °C); (b) CoCrTa(400 Å, room temperature)/Cr(600 Å, 260 °C), no sputter etching applied between layers; (c) CoCrTa(400 Å, room temperature)/Cr(300 Å, room temperature)/Cr(300 Å, 260 °C)/Cr no sputter etching between Cr layers.

but the NiP/Al disks are much better thermal and electrical conductors. Since the thermal conductivity of NiP/Al is 2 orders of magnitude higher than that of the Corning glass, the NiP/Al substrate can reach thermal equilibrium more easily and the heat can be more easily conducted away from the NiP/Al to the base plate. On the other hand, the thermally insulated glass could maintain a high temperature on the surface. Thus, this difference in thermal conductivity between NiP/Al and the Corning glass could very well cause the difference in the effect of bias on H_c .

To verify this idea, a Corning 7059 glass was inserted between the NiP/Al substrates and the base plate to reduce the heat transfer from NiP/Al substrate to the base plate. Another NiP/Al substrate, mechanically polished to one fourth of the original thickness (2 mm) to reduce its thermal mass, was also placed on the glass. A schematic of the ex-

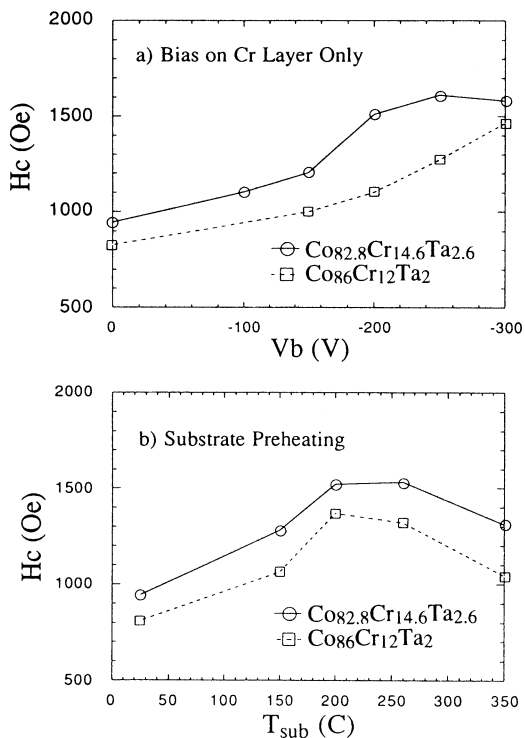


FIG. 6. H_c dependence of CoCrTa(400 Å)/Cr(600 Å) films on rf bias voltage and preheat substrate temperature. The bias was applied only during deposition of the Cr underlayer. The substrate was 7059 Corning glass.

periment is shown in Fig. 7. As can be seen in Table II, a significant enhancement in H_c was observed by reducing the heat transfer from the NiP/Al to the base plate. Also, the H_c was further increased when the thermal mass of the NiP/Al substrate was reduced to one fourth. The electroplated amorphous NiP layer was crystallized and became ferromagnetic at $V_b = -250$ V when the NiP/Al was further reduced to one tenth of its original thickness. Since the crystallization temperature of amorphous NiP is approximately 300 °C, this demonstrates that a high T_{sub} can be reached using NiP/Al substrates by bias sputtering the Cr underlayer when the NiP/Al is thermally isolated.

In the case of the glass substrates, we believe that the top surface had a much higher temperature than the rest of the substrate as a result of the bias sputtering. For the CoCrTa media the first order effect of achieving high H_c is to induce high atomic mobility, either by heating the substrate or perhaps by applying a bias which of course also heats the sub-

TABLE II. H_c of three Co_{82.8}Cr_{14.6}Ta_{2.6}(400 Å)/Cr(600 Å) films deposited on mechanically textured NiP/Al substrates (7 mm×7 mm) with varying thermal contact with base plate and thermal mass. The bias voltage during the sputtering of the Cr underlayer was -250 V.

Sample No.	Substrate thickness (mm)	Position	H_c (Oe)
		direct contact	
NiP/Al 1	2	with S.S. base plate	1280
NiP/Al 2	2	on 7059 glass	1670
NiP/Al 3	0.5	on 7059 glass	1780

strate. This may explain why NiP/Al disks require much higher bias voltage on Cr underlayers than glass disks to reach similar H_c when the substrates are isolated.

Our experiments have demonstrated that bias sputtering of Cr underlayers can produce similar high H_c media, just as preheating the substrates does. Although ΔM values were all significantly reduced by either bias sputtering of the Cr underlayers or preheating the substrate, the ΔM curves reveal different characteristics (Fig. 8). Therefore, different recording performance is probably expected for the media prepared by bias sputtering and preheating even though they have the same H_c . The variation may be a result of a variation in the microstructure of the films produced by the two techniques.

D. Composition effect and bias sputtering of the CoCrTa layer

For the two ternary CoCrTa targets used in our study, the M_s of the Co rich target (Co₈₆Cr₁₂Ta₂) was 30% higher than that of the Co_{82.8}Cr_{14.6}Ta_{2.6} target. Accordingly, the Co₈₆Cr₁₂Ta₂/Cr films had a higher M_s and remnant magnetization than the Co_{82.8}Cr_{14.6}Ta_{2.6}/Cr films for similar loop squareness (S).

Apart from the M_s , the composition difference in the CoCrTa targets gave different H_c dependence on bias voltage, where the bias was applied during Cr deposition only, and on the preheated substrate temperature (Fig. 6). The lower Co concentration films (Co_{82.8}Cr_{14.6}Ta_{2.6}/Cr) had much higher H_c than the Co richer films for a given T_{sub} , as they had a lower M_s . A higher density of faults and more solute segregation in the Co deficient film for a given T_{sub} may be responsible for the higher H_c .³

In order to increase the H_c of Co₈₆Cr₁₂Ta₂(400 Å)/Cr(600 Å) films, bias sputtering was employed while depositing the magnetic layer as well as bias sputtering of the Cr underlayer. As a result, H_c of the Co₈₆Cr₁₂Ta₂/Cr films increased with the bias voltage as shown in Fig. 9(a). At the

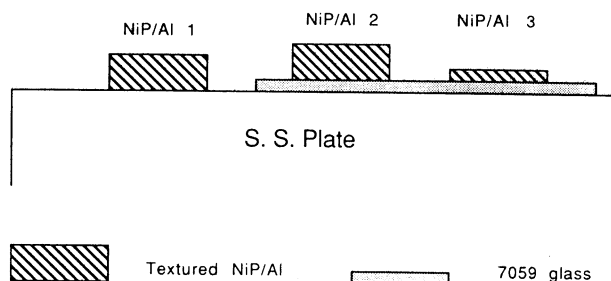


FIG. 7. Schematic depicting the experiment to study the heating effect caused by rf bias sputtering of the Cr underlayer.

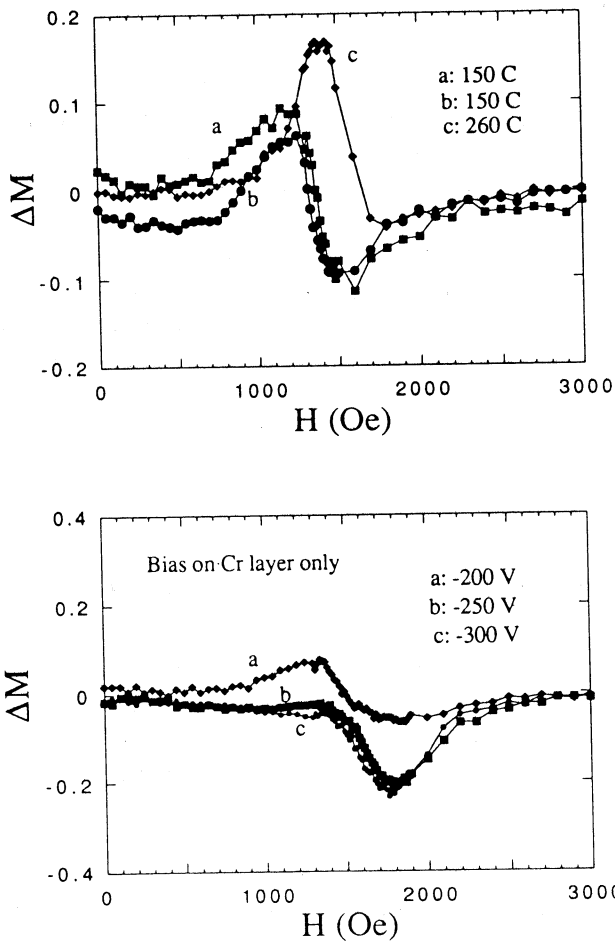


FIG. 8. ΔM curves of the films prepared by substrate preheating and bias sputtering of Cr underlayers.

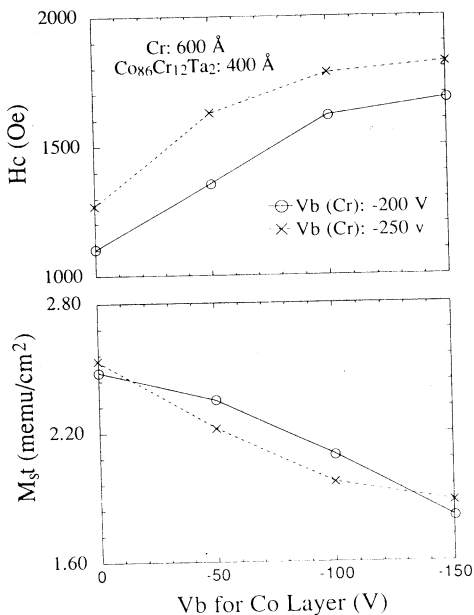


FIG. 9. The H_c and $M_s t$ dependence of $\text{Co}_{86}\text{Cr}_{12}\text{Ta}_2(400 \text{ \AA})/\text{Cr}(600 \text{ \AA})$ on bias voltage applied to the magnetic layer.

same time, the saturation magnetization for the same thickness of CoCrTa films decreased with the bias voltage as shown in Fig. 9(b). This indicates that the Co concentration of CoCrTa films decreased with the bias voltage. In addition to the effect of increasing the Cr and Ta concentration, bias sputtering of the magnetic layer enhanced the atomic mobility during the growth of the magnetic layer. Both of these effects would promote a high density of faults and solute segregation, leading to higher H_c . Recently, Deng *et al.* have measured the film composition by x-ray fluorescence and observed composition changes in bias sputtered CoCrTa films.¹³ In contrast to the method of bias sputtering on both the underlayer and the magnetic layer, Murata *et al.* combined preheating with bias sputtering of the magnetic CoCrTa layer. High H_c CoCrTa/Cr (>2000 Oe for 300 Å CoCrTa film) were produced.¹⁴ We believe that the same mechanism is involved.

IV. CONCLUSIONS

In summary, our studies in the processing and magnetic properties of CoCrTa/Cr longitudinal recording media have shown the following:

- (1) High H_c and low noise media can be obtained by either preheating the substrate or by rf bias sputtering. Bias sputtering of CoCrTa layer will increase H_c at the expense of decreasing the $M_s t$. The optimum processing conditions depend on the target composition.
- (2) The crystallographic texture of CoCrTa films (~ 500 Å) is controlled by the crystallographic texture of Cr underlayers regardless of T_{sub} . A clean Cr surface is essential to obtain high H_c and low noise media (in these experiments).
- (3) The enhancement in H_c at elevated T_{sub} is mainly controlled by elevated T_{sub} and is not dominated by the crystallographic texture, grain size, or the film stress.
- (4) T_{sub} has a pronounced effect on ΔM . The ΔM curves show that the elevated T_{sub} reduces significantly the intergranular exchange interaction. The Co/Cr crystallographic texture also has a measurable effect on ΔM . Based on our ΔM measurements it appears that the $\{1\bar{1}01\}_{\text{Co}}/\{110\}_{\text{Cr}}$ textured films should have better noise properties than the film with $\{11\bar{2}0\}_{\text{Co}}/\{200\}_{\text{Cr}}$ texture for similar H_c .

ACKNOWLEDGMENTS

The authors wish to thank Y. Deng at Carnegie Mellon University for a valuable discussion. The financial support of Hitachi Metals, Inc. for this research is gratefully acknowledged. The facilities used for this research are in part supported by the National Science Foundation under grant No. ECD-8907068.

- ¹A. Kawamoto, F. Hikami, S. Yasuda, and N. Muto, IEEE Trans. Magn. Mag. **27**, 5046 (1991).
- ²J. C. Lin, C. D. Wu, and J. M. Sivertsen, IEEE Trans. Magn. Mag. **26**, 39 (1990).
- ³Y. Shen, B. Y. Wong, and D. E. Laughlin, J. Appl. Phys. **76**, 8174 (1994).
- ⁴K. O'Grady, IEEE Trans. Magn. Mag. **26**, 1570 (1990).
- ⁵P. I. Mayo, K. O'Grady, R. W. Chantrell, J. A. Cambridge, I. L. Sanders,

- T. Yogi, and J. K. Howard, *J. Magn. Magn. Mater.* **95**, 109 (1991).
- ⁶R. Glang, R. A. Holmwood, and R. L. Rosenfeld, *Rev. Sci. Instrum.* **36**, 7 (1965).
- ⁷J. A. Christner, R. Ranjan, R. L. Peterson, and J. I. Lee, *J. Appl. Phys.* **63**, 3260 (1988).
- ⁸Y. Shen, D. E. Laughlin, and D. N. Lambeth, *IEEE Trans. Magn.* **28**, 3261 (1992).
- ⁹H. Hono, B. Wong, and D. E. Laughlin, *J. Appl. Phys.* **68**, 4734 (1990).
- ¹⁰H. C. Tsai, B. B. Lal, and A. Eltoukhy, *J. Appl. Phys.* **71**, 3579 (1992).
- ¹¹M. Lu, T. Min, Q. Chen, and J. H. Judy, *IEEE Trans. Magn.* **28**, 3225 (1992).
- ¹²B. Y. Wong and D. E. Laughlin, *Appl. Phys. Lett.* **61**, 2533 (1992).
- ¹³Y. Deng, D. N. Lambeth, X. Sui, L. Lee, and D. E. Laughlin, *J. Appl. Phys.* **73**, 5557 (1993).
- ¹⁴H. Murata, S. Fujii, H. Kogure, and T. Shinohara, *J. Magn. Soc. Jpn.* **15**, 672 (1991).